ELSEVIER

European Journal of Pharmaceutics and Biopharmaceutics 54 (2002) 51–58

European Journal of Pharmaceutics and Biopharmaceutics

www.elsevier.com/locate/ejphabio

Research paper

Determination of lipophilicity of two quinolone antibacterials, ciprofloxacin and grepafloxacin, in the protonation equilibrium

Jin Sun[a,b], Shigeko Sakai[a], Yoshihiko Tauchi[a], Yoshiharu Deguchi[a], Jimin Chen[b], Ruhua Zhang[b], Kazuhiro Morimoto[a,*]

[a]*Department of Pharmaceutics, Hokkaido College of Pharmacy, Otaru, Hokkaido, Japan*
[b]*Department of Pharmaceutics, Shenyang Pharmaceutical University, Shenyang, China*

Received 11 October 2001; accepted in revised form 30 January 2002

Abstract

The objective of this study was to compare protonation equilibrium and lipophilicity of two quinolone antibacterials, grepafloxacin (GPFX) and ciprofloxacin (CPFX), in order to give an insight into effects on the physicochemical properties by slight structural motifs. The protonation equilibrium was investigated by a spectrophotometry. Macro- and micro-dissociation constants were simultaneously determined, based on nonlinear regression analysis using the MULTI program, and then microspecies distribution could be described accordingly. Zwitterionic microspecies predominated at isoelectrical point (p*I*) for both drugs, and the concentration ratio of neutral to zwitterionic forms was near 4-fold greater for GPFX than that for CPFX. The apparent partition coefficient ($D_{O/B,pH}$) versus pH profiles had the shape of a parabolic curve in an *n*-octanol/buffer system, and reached the maximum around p*I* for both, respectively. Moreover, two introduced methyl groups in GPFX increased not only intrinsic lipophilicity but also neutral microspecies fraction relative to CPFX, and $D_{O/B,pH}$ of GPFX was consequently far higher than that of CPFX. The results emphasized that there were significant differences in protonation equilibrium and lipophilicity between GPFX and CPFX, which conduced to explaining their different behavior in terms of antibacterial activities and pharmacokinetics.

Keywords: Grepafloxacin; Ciprofloxacin; Microdissociation constant; Protonation equilibrium; Lipophilicity

1. Introduction

Grepafloxacin (GPFX) is one of newly synthesized quinolone antibiotics, exhibiting expanded antibacterial spectra, superior biological activity and excellent pharmacokinetics. As compared with ciprofloxacin (CPFX), GPFX possesses the similar chemical structure, but has two additionally introduced methyl groups in position 5 of quinoline ring and position 3′ of piperazinyl substituent, respectively (Fig. 1).

It is this slightly and subtly structural modification that has resulted in many antibacterial advantages for GPFX. Comparative studies of in vitro activity have shown that GPFX is as effective as CPFX against Gram-negative organism but better than CPFX against most Gram-positive bacteria, especially for *Streptococcus pneumoniae* and *Staphylococcus aureus* [1,2]. The penetration into *S. aureus* of GPFX is more efficient than that of CPFX [3]. Furthermore, GPFX has far more extensive tissue distribution than CPFX [4,5], in particular for the lung [6,7].

Results of structure–activity relationships indicate that the hydrophobic, electrical and steric parameters of quinolones play equally important roles in their biological activity [8]. The lipophilicity influences the penetration of quinolones into bacteria [9,10], and affects the intestinal absorption and membrane permeability. It may be reasonably expected that the significant differences in biological activities and pharmacokinetics between CPFX and GPFX, be ascribed to their dissimilar physicochemical properties resulting from alike chemical structures. Therefore, in the present study, we investigated the protonation equilibrium using the spectrophotometry from the macroscopic and microscopic standpoints, and studied pH-dependence in the partition behavior using an *n*-octanol/buffer system for GPFX and CPFX, in order to compare their physicochemical properties and to explore the consequences of two added methyl groups on the antibacterial activities and pharmacokinetics.

* Corresponding author. Department of Pharmaceutics, Hokkaido College of Pharmacy, 7-1 Katsuraoka-cho, Otaru-city, Hokkaido 047-0264, Japan. Tel.: +81-134-62-1848; fax: +81-134-62-1848.
E-mail address: morimoto@hokuyakudai.ac.jp (K. Morimoto).

0939-6411/02/$ - see front matter
PII: S0939-6411(02)00018-8

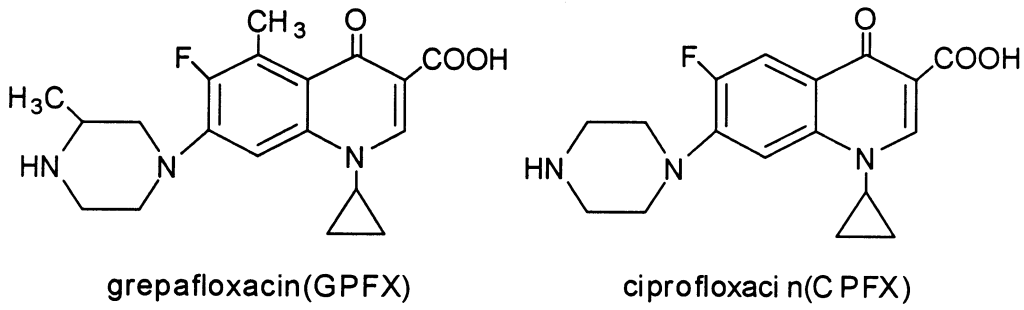

Fig. 1. Chemical structures of GPFX and CPFX.

2. Materials and methods

2.1. Materials

GPFX, CPFX, and OPC-17203 (internal standard for high-performance liquid chromatography (HPLC) assay) were synthesized and provided by Otsuka Pharm. Co. Ltd. (Tokyo, Japan). All other reagents were at least analytical grade.

2.2. Spectrophotometric measurement of protonation equilibrium

Three aliquots of 40 μM quinolone solutions were prepared in either 0.03 M NaH_2PO_4, 0.03 M Na_2HPO_4, or 0.03 M Na_3PO_4, with a total ionic strength of 0.2 M using NaCl. The solutions of different designated pH values were obtained by mixing three stock solutions. The pH measurements were undertaken by pH-meter (Horiba, pH-meter F-21, Japan), calibrated with three standards of pH 4.00, 7.00 and 9.00. The absorbance of the resulting solutions at selected wavelengths was determined and recorded using a spectrophotometer (DU-650, Beckman Instrument, Inc., Fullerton, CA, USA). Each determination was performed in duplicate at 25 °C.

2.3. Determination of apparent partition coefficient

The apparent partition coefficient in an *n*-octanol/buffer system was defined as $D_{O/B,pH}$ and measured by the shake-flask technique. The phosphate buffer solutions of different pH values containing 2 μM quinolones were prepared as described above and pre-saturated with *n*-octanol. The equal volumes (2 ml) of the aqueous and organic phases (presaturated with appropriate phosphate buffer solutions) were mixed and shaken at 25 °C for 4 h, by which the partitioning equilibrium was reached confirmed in the pilot study. Then, the samples were centrifuged ($700 \times g$) and two phases separated. One-hundred-milliliter specimens of both phases were sampled, added to 100 μl internal standard solution (0.5 μM OPC-17203 in methanol) and 400 μl methanol for dilution, and 40-μl aliquots were subjected into HPLC system, respectively. Each determination was conducted in duplicate.

2.4. HPLC analysis

The HPLC system (Shimadazu, Kyoto, Japan) consisted of an LC-10AD pump, RF-$10A_{XL}$ fluorescence detector, CTO-6A oven, C-R6A data process integrator, and an STR ODS-II column (5 μm, 4.0×250 mm, Shinwa Chemical Co., Kyoto, Japan). Mobile phase was composed of 0.01% phosphoric acid (containing 20 mM Na_2SO_4)–acetonitrile (3:1, v/v). The flow rate was 0.8 ml/min and the column temperature was 40 °C. The eluate was monitored using the fluorescence detector ($\lambda_{ex} = 325$ nm, $\lambda_{em} = 448$ nm for both GPFX and CPFX).

2.5. Curve-fitting calculation

The curve-fitting calculation to obtain the 'best' microscopic and macroscopic constants as judged by the least squares criterion was performed with the program MULTI [11]. The input data were weighted as the reciprocal of the observed values and the Damping Gauss Newton method was used for the fitting algorithm. The uncertainties reported with the constants were linear estimates of the standard deviation, as calculated by MULTI.

3. Results and discussion

3.1. Comparison and evaluation of protonation equilibrium of CPFX and GPFX

The amphoteric quinolones, such as GPFX and CPFX, contain two proton-binding sites, of which micro-dissociation constants differ within several orders of magnitude. The deprotonation of two proton-binding groups to a certain extent overlaps, and they accordingly exist as four microspecies in solution, namely positive, zwitterionic, neutral and negative forms at the molecular level [12–14]. In addition, macro-dissociation constant is a complex of micro-dissociation constants and cannot be assigned to the individual group. The macroscopic and microscopic protonation equilibria of GPFX are described in Fig. 2.

The proton-binding ability of the individual group is characterized by the micro-dissociation constants (k_1, k_2, k_{12}, k_{21}), defined as (Fig. 2):

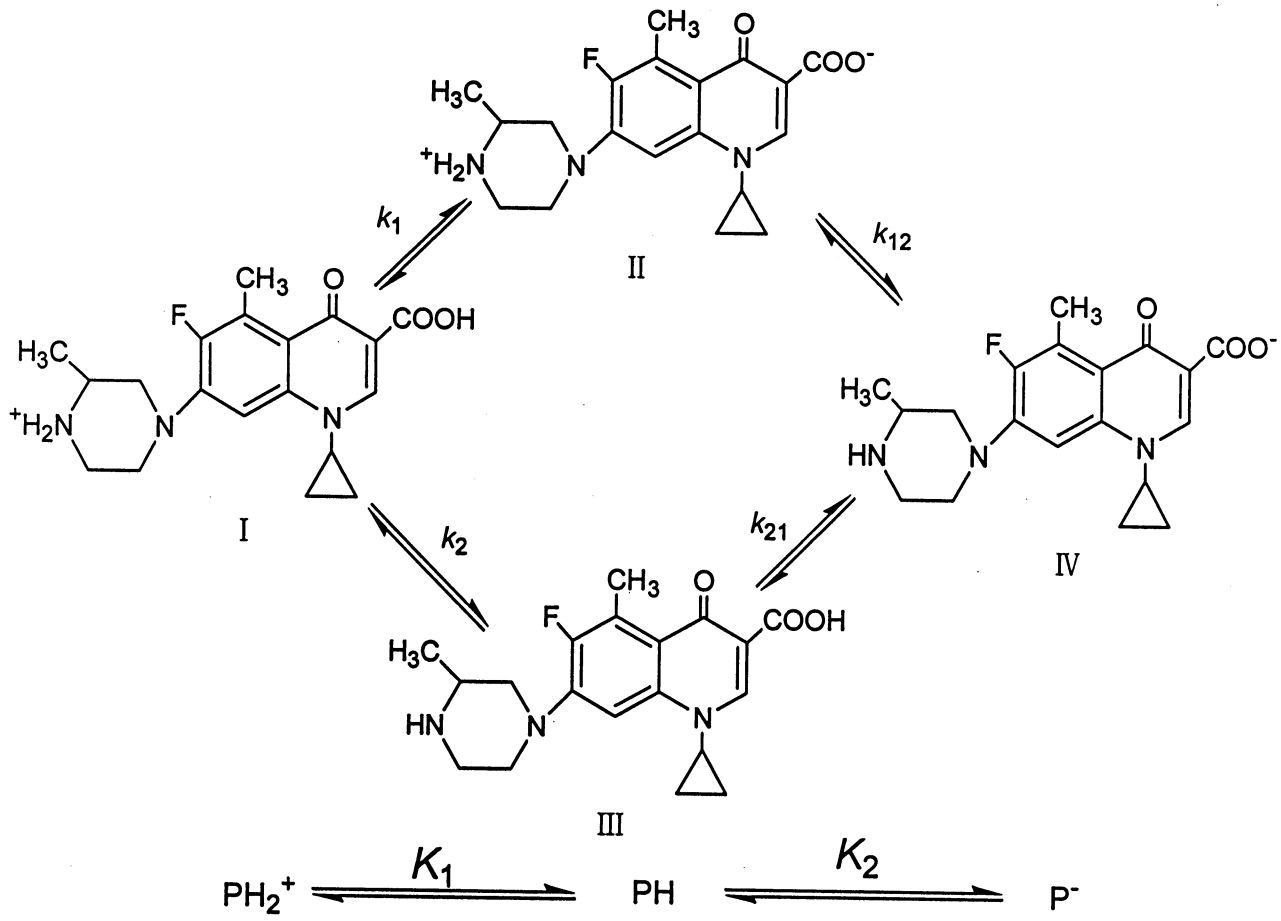

Fig. 2. Macro- and micro-protonation equilibria of GPFX. I, II, III and IV represent the positive, zwitterionic, neutral and negative microspecies, respectively. k_1, k_2, k_{12}, k_{21} are micro-dissociation constants of the individual group. PH_2^+ represents cationic species, PH represents zwitterionic species, and P^- represents the anionic specie, respectively. K_1 and K_2 are stepwise macro-dissociation constants.

$$k_1 = \frac{[\mathrm{II}][\mathrm{H}^+]}{[\mathrm{I}]} \tag{1}$$

$$k_2 = \frac{[\mathrm{III}][\mathrm{H}^+]}{[\mathrm{I}]} \tag{2}$$

$$k_{12} = \frac{[\mathrm{IV}][\mathrm{H}^+]}{[\mathrm{II}]} \tag{3}$$

$$k_{21} = \frac{[\mathrm{IV}][\mathrm{H}^+]}{[\mathrm{III}]} \tag{4}$$

where I, II, III and IV represent the positive, zwitterionic, neutral and negative microspecies, respectively.

The macro-dissociation constants (K_1, K_2) are expressed as (Fig. 2):

$$K_1 = \frac{[\mathrm{PH}][\mathrm{H}^+]}{[\mathrm{PH}_2^+]} = \frac{([\mathrm{II}] + [\mathrm{III}])[\mathrm{H}^+]}{[\mathrm{I}]} \tag{5}$$

$$K_1 = \frac{[\mathrm{P}^-][\mathrm{H}^+]}{[\mathrm{PH}]} = \frac{[\mathrm{IV}][\mathrm{H}^+]}{[\mathrm{II}] + [\mathrm{III}]} \tag{6}$$

where PH_2^+ represents cationic species corresponding to positive microspecies, PH represents zwitterionic species including zwitterionic and neutral microspecies, and P^- represents the anionic species corresponding to negative microspecies, respectively.

Taken together, the relationships between the micro- and macro-dissociation constants are:

$$K_1 = k_1 + k_2 \tag{7}$$

$$1/K_2 = 1/k_{12} + 1/k_{21} \tag{8}$$

$$K_1 K_2 = k_1 k_{12} = k_2 k_{21} \tag{9}$$

Note that, among six micro- and macro-dissociation constants, only three parameters are independent due to their relationships of three unrelated equations (7–9).

The spectrophotometry is chose to investigate the micro-protonation equilibrium because pH-dependent UV absorption spectra of quinolones depend on the protonation state of carboxyl group, but independent of that of piperazinyl moiety [13]. Additionally, the acid form of carboxyl group can differ markedly from its conjugated base as far

as the UV spectra are concerned. For these reasons, the deprotonation fraction of the carboxyl group for quinolones can be determined sensitively and specifically by measuring the pH-dependent UV spectra.

As for UV spectra of GPFX in Fig. 3, isosbestic points were observed in the pH-dependent absorbance–λ profiles and UV spectra were solely influenced by the protonation state of carboxyl group in the absorbance-pH profiles. In addition, the contour in UV spectra of CPFX was similar to that of GPFX (unpublished data). Then, the deprotonation fraction of carboxyl group for two studied drugs could be calculated from pH-dependent absorbance:

$$\alpha_{COO^-(pH)} = \frac{A_{(pH)} - A_{(COOH)}}{A_{(COO^-)} - A_{(COOH)}} \quad (10)$$

Where $A_{(COO^-)}$ and $A_{(COOH)}$ are experimental absorbance values when carboxyl group is deprotonated and protonated, respectively, and $\alpha_{COO^-(pH)}$ is the deprotonation fraction of carboxyl moiety at the certain pH where absorbance is $A_{(pH)}$. In this study, $\alpha_{COO^-(pH)}$ values of GPFX and CPFX were calculated at five wavelengths (278-290 nm) where there existed the larger variations in absorbance between acidic and conjugated basic forms, and were expressed as the mean.

As shown in Fig. 2, the degree of deprotonation in carboxyl group is also described by arranging the equations (1–6):

$$\alpha_{COO^-(pH)} = \frac{[II] + [IV]}{[I] + [II] + [III] + [IV]} = \frac{k_1[H^+] + K_1K_2}{[H^+]^2 + K_1[H^+] + K_1K_2} \quad (11)$$

The dissociation constants K_1, K_2 and k_1 could be calculated by an iterative nonlinear least squares analysis from the data of $\alpha_{COO^-(pH)}$ versus pH according to Eq. (11), using MULTI program [11]. Plots of predicted $\alpha_{COO^-(pH)}$ versus pH are shown in Fig. 4 to illustrate the good fit with experimental data. This method was based on nonlinear regression of the deprotonation fraction of quinolone carboxyl group as a function of pH, and simultaneously determined macro- and micro-constants that came from the same experiment. However, the approach exploited by Takacs-Novak required two separate experiments for determining macro- and micro-constants, respectively, and was difficult to assure the same experimental condition [13]. The other micro-dissociation constants (k_2, k_{12}, k_{21}) were calculated according to Eqs. (7–9) and the resulting values are listed in Table 1.

The pK_1 and pK_2 values of GPFX and CPFX are similar to values previously reported [15,16], and mainly represent the basicity of carboxyl and piperazinyl amino groups, respectively. There is no difference in pK_2 between both, indicating that the basicity of amino group is not affected by introducing 3′-methyl group in GPFX. By contrast, pK_1 of

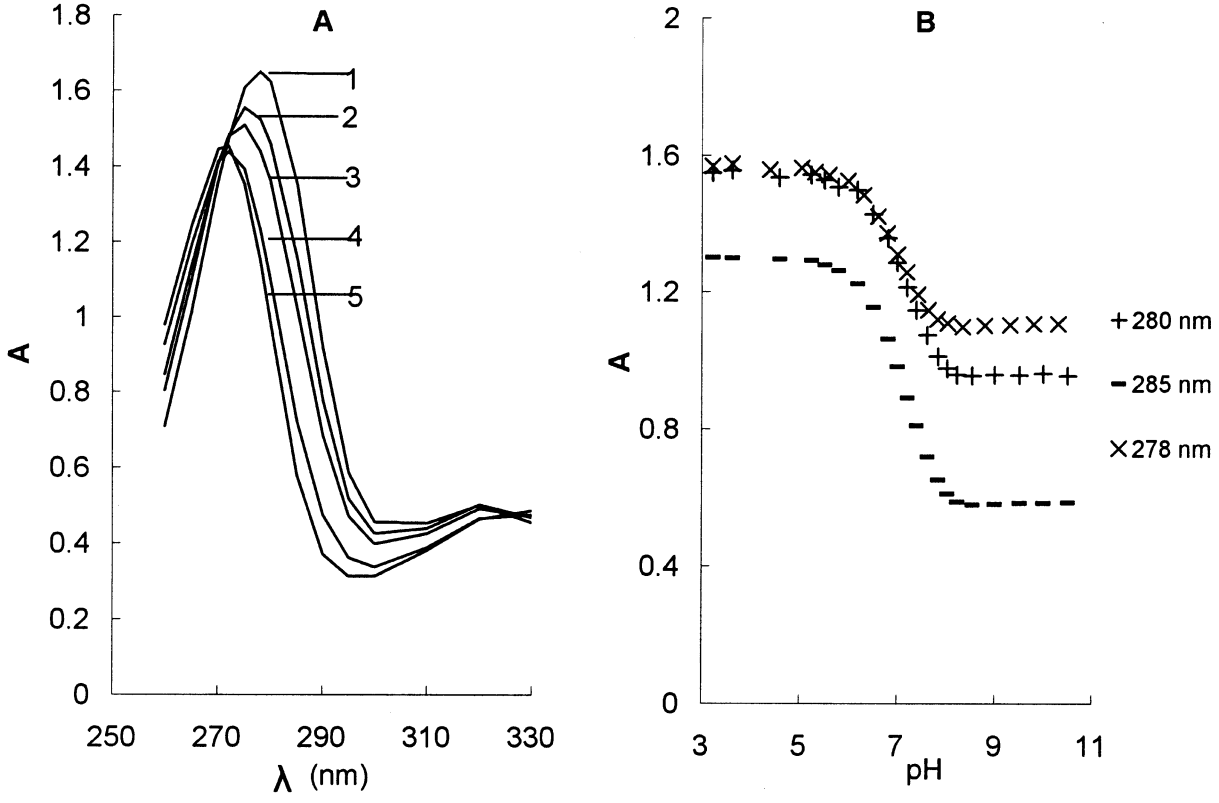

Fig. 3. pH-dependent UV spectra of GPFX. (A), absorbance versus λ curves, key: (1) pH 4.50; (2) pH 6.50; (3) pH 6.80; (4) pH 7.50; (5) pH 9.34. (B) Absorbance versus pH profiles.

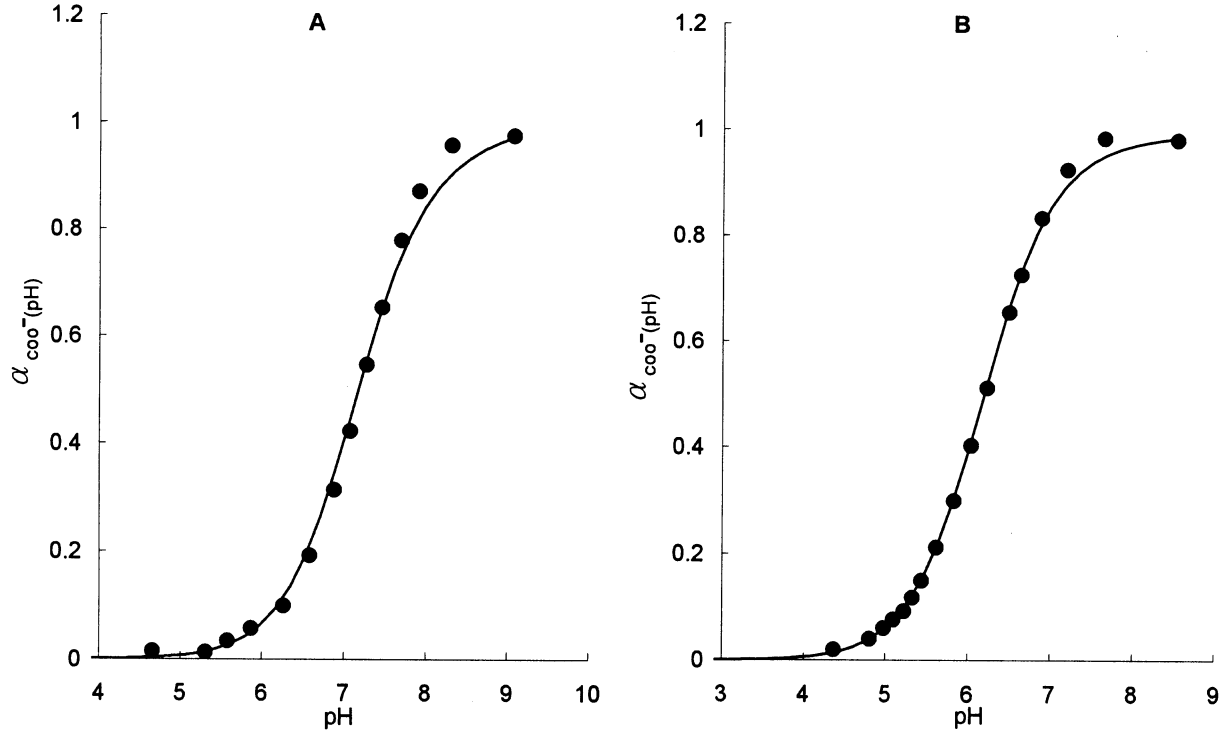

Fig. 4. $\alpha_{COO^-(pH)}$ versus pH profiles of GPFX and CPFX. Deprotonation fraction of carboxyl group ($\alpha_{COO^-(pH)}$ for GPFX and CPFX was determined at five wavelengths (278–290 nm) and expressed as the average. Solid lines showed the calculated $\alpha_{COO^-(pH)}$ versus pH profiles based on estimated constants. (A) GPFX; (B) CPFX.

GPFX is 1 unit greater than that of CPFX, demonstrating reduced acidity for GPFX which is due to the electron-donating effect by added 5-methyl group stabilizing the protonation state of the carboxyl group. Furthermore, both are weaker acids than either the aromatic carboxylic acids or the aliphatic β-ketocarboxylic acids. The intra-molecular hydrogen-bond formation between the carboxyl and keto groups in the quinoline ring contributes to lowered acidic character for quinolones, because of improved stability of the protonated form of the carboxyl group [13].

When comparisons are made of micro-constants belonging to the same proton-binding site (pk_1 and pk_{21}, pk_2 and pk_{12}), there are notably different values. This suggests that, in spite of lots of intervening atoms between two proton-binding sites, protonation at one site can markedly reduce the basicity of the other site ($pk_1 < pk_{21}$, $pk_2 < pk_{12}$) [13]. More importantly, the micro-protonation equilibrium, distribution of four microspecies, can be characterized in detail using these constants. The fractions of four microspecies in solution are calculated by:

$$f(I) = \frac{[H^+]^2}{[H^+]^2 + K_1[H^+] + K_1K_2} \quad (12)$$

$$f(II) = \frac{k_1[H^+]}{[H^+]^2 + K_1[H^+] + K_1K_2} \quad (13)$$

$$f(III) = \frac{k_2[H^+]}{[H^+]^2 + K_1[H^+] + K_1K_2} \quad (14)$$

$$f(IV) = \frac{K_1K_2}{[H^+]^2 + K_1[H^+] + K_1K_2} \quad (15)$$

Where f(I), f(II), f(III) and f(IV) denote the fractions of positive, zwitterionic, neutral and negative microspecies, respectively.

The four microspecies distribution for GPFX and CPFX is shown in Fig. 5. Evidently, the zwitterionic microspecies predominated at determined pI for both, which was close to physiological pH. Understanding microspecies distribution

Table 1
Macro- and micro-dissociation constants for GPFX and CPFX[a]

Constants	GPFX	CPFX
pK_1	7.12 (0.03), 7.10[b]	6.18 (0.01), 6.18[c]
pK_2	8.78 (0.03), 8.80[b]	8.73 (0.01), 8.66[c]
pk_1	7.15 (0.02)	6.19 (0.01)
pk_2	8.27 (0.03)	7.86 (0.01)
pk_{12}	8.75 (0.04)	8.72 (0.01)
pk_{21}	7.64 (0.03)	7.04 (0.01)
pI[d]	7.95	7.46

[a] Figures in parentheses represented standard deviation. The determination of constants was performed at ionic strength of 0.2 M at 25 °C.
[b] From Ref. [15].
[c] From Ref. [16].
[d] Calculated by $(pK_1 + pK_2)/2$ in this study.

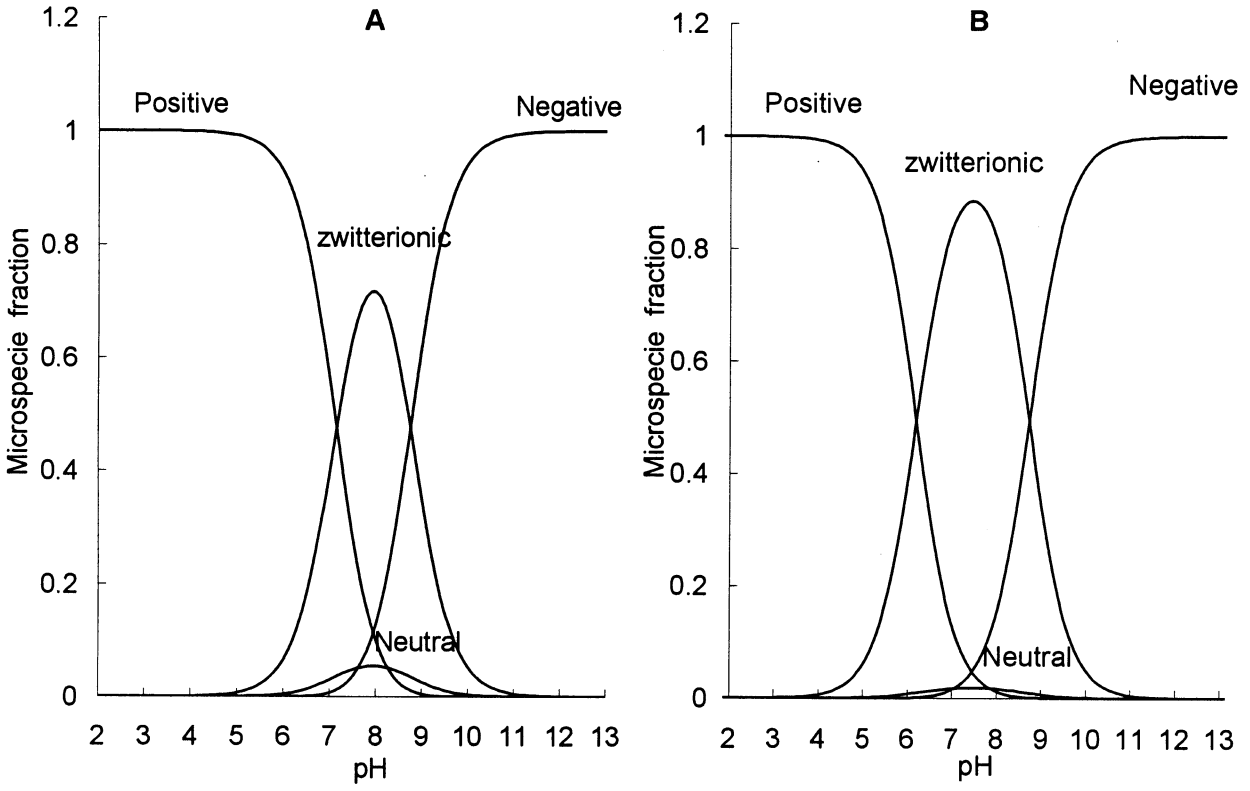

Fig. 5. Distribution of four microspecies. (A) GPFX; (B) CPFX.

is essential since the drug-receptor associations and drug–membrane interactions are involved in the molecule-molecule interaction with the complementary conformations. On the basis of microspecies distribution, explaining interactions between amphoteric quinolones and ordered phospholipid membrane will be discussed in a later report. A concentration ratio of neutral/zwitterionic forms of GPFX (7.64%) was near 4-fold greater than that for CPFX (2.09%), leading to reduced zwitterionic and increased neutral fractions for GPFX (Fig. 5). It had been found that the ratio varied greatly among the quinolones [13] and heavily influenced their apparent partition coefficients [17].

3.2. pH-Dependence in the apparent partition coefficient for GPFX and CPFX

In Fig. 6, log $D_{O/B,pH}$ versus pH profiles for GPFX and CPFX took the form of bell-shape and both peaks were reached at near p*I* of GPFX (7.95) and CPFX (7.46) determined in this study, respectively. Also, $D_{O/B,7.4}$ of GPFX (5.13) was 31-fold greater than that of CPFX (0.166), suggesting that GPFX was far more lipophilic than CPFX.

Recent studies had shown that GPFX uptake by human polymorphonuclear leukocytes achieved a maximum at pH around p*I* and demonstrated the similar contour to profile of log $D_{O/B,pH}$ versus pH [15]. This implied that the high apparent partition coefficient was associated with high membrane permeability and resulted in maximum uptake at p*I*. In addition, it was found that the antibacterial activity of GPFX was lowered when pH decreased from pH 8.0 to 6.0 [3]. These may have contributed to the p*I* of GPFX (7.95) which lies in basic region due to reduced acidity of 3-carboxyl group by

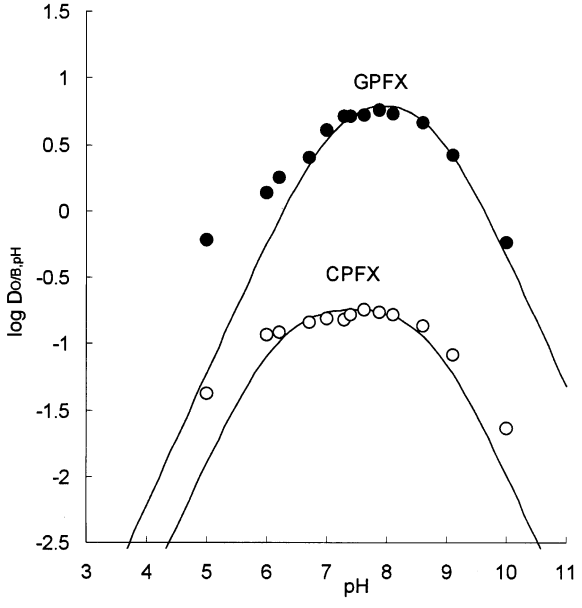

Fig. 6. Apparent partition coefficient of GPFX and CPFX in an *n*-octanol/buffer system. Solid lines represented the calculated log $D_{O/B,pH}$ versus pH profiles based on estimated log $P_{O/B}$ values.

addition of 5-methyl substituent as compared to CPFX. When pH declines from p*I*, $\log D_{O/B,pH}$ and membrane permeability will decrease (Fig. 6), and thus the penetration into bacteria will be impaired. Since the activity of quinolones depends on their inhibition of bacterial DNA gyrase, their entry into bacteria is a prerequisite for taking effect and so GPFX antibacterial activity is reduced.

The thermodynamic partition coefficient (intrinsic lipophilicity, $P_{O/B}$) is defined by distribution law:

$$P_{O/B} = [III]_o/III]_w \quad (16)$$

Where $[III]_o$ and $[III]_w$ represent concentrations of neutral microspecies in organic and aqueous phases, respectively.

On the other hand, the apparent partition coefficient ($D_{O/B,pH}$) is described by total concentrations of organic phase divided by those of aqueous phases. With respect to organic phase, the transfer for negative, positive and zwitterionic microspecies into it is unlikely due to the lower tendency of the organic solvent to solvate the polar ions compared with water [18]. Takacs-Novak et al. have provided experimental evidence for this assumption that only neutral microspecies can effectively partition into organic phase for amphoteric molecules [19]. On the contrary, there are four microspecies prevailing in dynamic equilibria and rapid conversion for amphoteric quinolones in aqueous phase. So, $D_{O/B,pH}$ was described by:

$$\begin{aligned} D_{O/B,pH} &= [III]_o/([I]_w + [II]_w + [III]_w + [IV]_w) \\ &= ([III]_o/[III]_w) \\ &\quad \times ([III]_w/([I]_w + [II]_w + [III]_w + [IV]_w)) \end{aligned} \quad (17)$$

Combining Eqs. (16) and (17) results in an equation concerning the relationship between $P_{O/B}$ and $D_{O/B,pH}$:

$$D_{O/B,pH} = P_{O/B} \times f(III) \text{ or } P_{O/B,pH} = D_{O/B}/f(III) \quad (18)$$

An ion-pair may be formed between the positive microspecies of quinolones and the negatively charged phosphate or chloride ions of buffer in an acidic environment [17]. Alternatively, the order of ability to form the ion-pair is primary > secondary > tertiary amino groups [20], and both GPFX and CPFX are belonging to secondary amine. Hence, both possess potential capability of forming an ion-pair, which can partition into *n*-octanol phase. So log $P_{O/B}$ values were calculated as the average at neutral pH in order to avoid the ion-pair effect, and were 2.05 ± 0.04 and 0.99 ± 0.05 for GPFX and CPFX, respectively. On the basis of known log $P_{O/B}$ and f(III) values, the plots of log $D_{O/B,pH}$ versus pH could be predicted using Eq. (18), as shown in Fig. 6, which illustrated the good agreement with experimental data under neutral and basic conditions but not acidic condition. It implied the formation of the ion-pair at acidic circumstance which allowed for partitioning of positive form into organic phase [17]. However, under basic conditions, the experimental log $D_{O/B,pH}$ of CPFX appeared to slightly deviate from the predicted values too. The underlying reason was unclear, perhaps due to either an ion-pair between negative form and cationic ion of buffer, or weak ingression of negative microspecies into *n*-octanol phase, because Irwin et al. reported that the anionic species of zwitterionic cephalosporin antibiotics could partition into organic phase [21].

Moreover, since the ratio of $D_{O/B,7.4}$ for GPFX to CPFX was about 31-fold while that of $P_{O/B}$ was just 11.2-fold., the ratio of neutral/zwitterionic forms exerted a larger effect on $D_{O/B,pH}$. That is to say, the apparent partition coefficient of quinolones was not only influenced by their intrinsic lipophilicity, but also markedly affected by their complex protonation equilibria. As both intrinsic lipophilicity and neutral fraction of GPFX were increased by two introduced methyl groups as compared to CPFX, $D_{O/B,pH}$ for GPFX was far higher than that for CPFX. This inferred that protonation equilibrium or neutral fraction should be concerned as an essential factor in the physicochemical property-based design of quinolones for improved lipophilicity.

The comparative structure–activity studies of GPFX and CPFX indicated that 5′- and 3′-piperazinyl methyl groups enhanced activity against Gram-positive bacteria, improved tissue penetration, and prolonged $t_{1/2}$ [22,23]. Taking the increased $D_{O/B,pH}$ by two methyl groups into account, the membrane permeability would be significantly enhanced, and consequently facilitated GPFX better penetrate into bacteria and distribute into tissue than CPFX. The extensive tissue distribution partly delayed the urinary excretion and hepatic metabolism, and probably contributed to prolonged $t_{1/2}$ of GPFX. Furthermore, Wakebe et al. reported that MIC against *S. aureus* of GPFX (0.05 μg/ml) was much lower than that of CPFX (0.39 μg/ml), but IC_{50} of inhibiting isolated *S. aureus* SA113 DNA gyrase for GPFX (23.0 μg/ml) was not lower than that for CPFX (20.5 μg/ml). In addition, they found that GPFX showed a higher uptake than CPFX in *S. aureus* and inferred that the activity against Gram-positive bacteria could be affected not only by the inhibition of DNA gyrase but also by the extent of accumulation of drug in the bacteria [3]. Therefore, the two introduced methyl groups of GPFX increased $D_{O/B,pH}$ and membrane permeability, and as a result improved accumulation within bacteria and enhanced activity against Gram-positive bacteria. In sum, clarification of effects on physicochemical properties and further on biologic activity and pharmacokinetics by added 5′- and 3′-methyl substituents will gain an insight into the design of new quinolone drugs for good antibacterial activities and pharmacokinetics.

4. Conclusion

The results demonstrated that there were significant differences in the protonation equilibrium and lipophilicity for GPFX and CPFX, as a result of slight structural motifs. The zwitterionic microspecies predominated near physiological pH and the concentration ratio of neutral/zwitterionic

forms of GPFX was greater than that of CPFX. Moreover, owing to increased both intrinsic lipophilicity and neutral fraction of GPFX by two added methyl groups relative to CPFX, $D_{O/B,pH}$ for GPFX was far larger than that for CPFX, which was beneficial to elucidate their different behavior in antibacterial activities and pharmacokinetics.

Acknowledgements

We are very grateful to the Otsuka Pharm. Co. Ltd. for donating the studied drugs and for a grant.

References

[1] M. Kimura, T. Kishimoto, Y. Niki, R. Soejima, In vivo and in vitro antichlamydial activities of newly developed quinolone antimicrobial agents, Antimicrob. Agents Chemother. 37 (1993) 801–803.
[2] R. Wise, J.M. Andrew, N. Brenwald, The in-vitro activity of OPC-17116, a new 5-methyl substituted quinolone, J. Antimicrob. Chemother. 31 (1993) 497–504.
[3] H. Wakebe, S. Mitsuhashi, Comparative in vitro activities of a new quinolone, OPC-17116, possessing potent activities against gram-positive bacteria, Antimicrob. Agents Chemother. 36 (1992) 2185–2191.
[4] K. Vance-Bryan, D.R.P. Guay, J.C. Rotschafer, Clinical pharmacokinetics of ciprofloxacin, Clin. Pharmacokinet. 19 (1990) 434–461.
[5] C. Efthymiopoulos, S.L. Bramer, A. Maroli, Pharmacokinetics of grepafloxcain after oral administration of single and repeat doses in healthy young males, Clin. Pharmacokinet. 33 (Suppl. 1) (1997) 1–8.
[6] T. Ito, I. Yano, S. Masuda, Y. Hashimoto, K. Inui, Distribution characteristics of levofloxacin and grepafloxacin in rat kidney, Pharm. Res. 16 (1999) 534–539.
[7] M. Murata, I. Tamai, Y. Sai, O. Nagata, H. Kato, A. Tsuji, Carrier-mediated lung distribution of HSR-903, a new quinolone antibacterial agent, J. Pharmacol. Exp. Ther. 289 (1999) 79–84.
[8] M. Ohta, H. Koga, Three-dimensional structure–activity relationships and receptor mapping of N_1-substituted of quinolone antibacterials, J. Med. Chem. 34 (1991) 131–139.
[9] G.E. Stein, The 4-quinolone antibiotics: past, present, and future, Pharmacotherapy 8 (1988) 301–304.
[10] L.J.V. Piddock, M.C. Hall, R. Wise, Mechanism of action of lomefloxacin, Antimicrob. Agents Chemother. 34 (1990) 1088–1093.
[11] K. Yamaoka, Y. Tanigawara, Y. Nakagami, T. Uno, A pharmacokinetic analysis program (MULTI) for microcomputer, J. Pharmacobio-Dyn. 4 (1981) 879–885.
[12] S. Riegelman, L.A. Strait, E.Z. Fischer, Acid dissociation constants of phenylalkanolamines, J. Pharm. Sci. 51 (1962) 129–133.
[13] K. Takacs-Novak, B. Noszal, I. Hermecz, G. Kereszturi, B. Podanyi, G. Szasz, Protonation equilibria of quinolone antibacterials, J. Pharm. Sci. 79 (1990) 1023–1028.
[14] B. Noszal, Statistical mechanics and thermodynamics. Group constant: A measure of submolecular basicity, J. Phys. Chem. 90 (1986) 4104–4110.
[15] K. Taira, H. Koga, S. Kohno, Accumulation of a newly developed fluroquinolone, OPC-17116, by human polymorphonuclear leukocytes, Antimicrob. Agents Chemother. 37 (1983) 1877–1881.
[16] K.E. Brighty, T.D. Gootz, The chemistry and biological profile of trovafloxacin, J. Antimicrob. Chemother. 39 (Suppl. B) (1997) 1–14.
[17] D.L. Ross, S.K. Elkinton, C.M. Riley, Physicochemical properties of the fluroquinolone antibacterials III: 1-octanol/water partition coefficients and their relationships to structure, Int. J. Pharm. 88 (1992) 379–389.
[18] K. Takacs-Novak, M. Jozan, I. Hermecz, G. Szasz, Lipophilicity of antibacterial fluroquinolones, Int. J. Pharm. 79 (1992) 89–96.
[19] K. Takacs-Novak, M. Jozan, G. Szasz, Lipophilicity of amphoteric molecules expressed by the true partition coefficient, Int. J. Pharm. 113 (1995) 47–55.
[20] M.M. Davis, M. Paabo, Acid-base equilibria in benzene at three temperatures. The comparative reactivities of a phenolic acid and a carboxylic acid with triethylamine and with 1,3-diphenylguanidine, J. Am. Chem. Soc. 82 (1960) 5081–5084.
[21] V.P. Irwin, J.M. Quigley, R.F. Timoney, 1-Octanol–water partition coefficients of the anionic and zwitterionic species of diprotic zwitterionic cephalosporin antibiotics, Int. J. Pharm. 43 (1988) 187–188.
[22] H.C. Neu, Chemical evolution of the fluoroquinolone antimicrobial agent, Am. J. Med. 87 (Suppl. 6c) (1989) 2s–9s.
[23] G.S. Tillotson, Quinolones: structure–activity relationships and future prediction, J. Med. Microbiol. 44 (1996) 320–324.